2018:00218- Unrestricted

Report

Reconstruction of a distributed energy balance snow pack model

A deliverable from the SnowHow project

Author(s)
Sjur Anders Kolberg

SINTEF Energy Research
Water Resources
2018-02-20

SINTEF Energi AS
SINTEF Energy Research
Address:
Postboks 4761 Sluppen
NO-7465 Trondheim
NORWAY
Switchboard: +47 73597200
Telefax: +47 73597250
energy.research@sintef.no
www.sintef.no/energi
Enterprise /VAT No:
NO 939 350 675 MVA

KEYWORDS:
Hydrology
Inflow modelling
Snow
Albedo

Report

Reconstruction of a distributed energy balance snow pack model

A deliverable from the SnowHow project

VERSION
1.1

DATE
2018-02-20

AUTHOR(S)
Sjur Anders Kolberg

CLIENT(S)
Norwegian Research Council

CLIENT'S REF.
NFR 244153 ThS

PROJECT NO.
502001057

NUMBER OF PAGES/APPENDICES:
28 / 0

ABSTRACT
This report describes the construction of the second generation snow pack model GamSnow, used to simulate snow melt in a distributed hydrological model. The work has been carried out as a part of the SnowHow project, supported by the Norwegian Research Council under the KLIMAFORSK programme.

The main novelties in the new snow model is a new albedo formulation, and an improved approach to simulating snow surface temperature. Motivated by increased physical coherence and less dependency on calibration, these changes have improved the model's correspondence to measurements, despite reducing the number of free parameters. Compared to the original model, the parameters in the new formulation are better identified during estimation, and the optimal values for simulating discharge and snow coverage are in better agreement.

This indicates that physically based modelling can avoid the tendency of being overly sensitive to poorly known quantities, and justify its use both in operational water management and in climate studies where stationarity is questionable.

PREPARED BY Sjur Kolberg	**SIGNATURE** Sjur Kolberg
CHECKED BY Julie Charmasson	**SIGNATURE** J Charmasson
APPROVED BY Knut Samdal	**SIGNATURE** Knut Samdal

REPORT NO.	**ISBN**	**CLASSIFICATION**	**CLASSIFICATION THIS PAGE**
2018:00218	978-82-14-06640-1	Unrestricted	Unrestricted

Document history

VERSION	DATE	VERSION DESCRIPTION
1.0	2018-02-19	First version
1.1	2018-02-20	Quality controlled

SINTEF

Table of contents

1 Introduction **4**

2 Model description **4**

2.1 Spatial distribution 5

2.2 Necessary inputs 5

2.3 Simulated responses 5

2.4 The melt equation 6

2.4.1 Shortwave radiation 7

2.4.2 Longwave radiation 7

2.4.3 Turbulent energy flux 7

2.4.4 Internal energy and liquid water content 7

2.5 Sub-grid snow distribution 7

2.6 Runoff from glaciers 9

3 A new albedo formulation **9**

3.1.1 Grain size modelling, dry snow 10

3.1.2 Grain size modelling, wet snow 13

3.1.3 Albedo model 14

4 Results **16**

4.1 Experiment setup 16

4.2 Calibration results and performance statistics: 17

4.2.1 Identifiability of albedo-model parameters 17

4.2.2 Identifiability of other snow model parameters 21

4.3 Differences in albedo model behaviour 22

4.4 Differences in longwave parameterization 22

4.5 Hydrological simulations 24

5 Conclusions **26**

Acknowledgements **26**

References: **27**

APPENDICES

[List appendices here]

1 Introduction

The following report describes the construction of the second generation snow pack model GamSnow, used to simulate snow melt in a distributed hydrological model. GamSnow was originally developed during 2000-2003, as a module in what later became the Enki modelling platform. It is today also a part of Statkraft's Hydrological Forecasting Toolbox (SHyFT), as well as Powel's Smart Generation (SmG) suite of water management and hydropower scheduling software, used by most larger hydropower producers in Scandinavia. This grid distributed model is now challenging the semi-distributed HBV model (Bergström and Forsman, 1973) as an operational tool in the Norwegian hydropower sector.

During the development of a distributed inflow model as an alternative to HBV, GamSnow was the first sub-routine to replace its HBV counterpart HBVSnow, which was originally based on elevation zones and a degree-day snowmelt principle. GamSnow extended the spatial distribution scheme to grid cells, and replaced the degree-day snowmelt equation with an energy budget approach. It was designed for multi-variable calibration and validation; and was used in a series of papers investigating the assimilation of remotely sensed snow cover information (e.g. Kolberg et al., 2006; Kolberg and Gottschalk, 2010).
At the core of GamSnow was the Snow Depletion Curve (SDC); replacing HBV's piecewise linear snow distribution function. The SDC concept has been discussed by, among others, Luce et al (1998) and Liston (1998); and its reconstruction from remotely sensed data by e.g. Durand et al., (2008). Based on extensive snow surveys, a Gamma model was selected for the probability density function underlying the SDC; hence the name of the routine.

As Enki continued to develop, more of its originally HBV-based routines were replaced by new and simpler formulations. The simplification in terms of number of parameters and state variables is considered necessary given the expanding from an elevation zone based to a grid based spatial distribution scheme. Eventually it became clear that the original GamSnow routine was by far the most complex routine in the model; and it indeed contained a number of parameters which were not identifiable during calibration.
A revision of GamSnow has therefore been desirable and was identified as a specific sub-objective for the SnowHow project. The ambition has been to strengthen its adherence to physical principles, to increase the observability of its internal states, and to reduce its dependency of calibration by removing poorly identifiable parameters.

2 Model description

The 2nd generation GamSnow routine is, as its predecessor, a grid distributed snow accumulation and melt model designed for hydrological modelling with emphasis on assimilating remotely sensed information. It employs a Snow Depletion Curve (SDC) to describe the small-scale heterogeneity in each grid cell. The purpose of the SDC is to keep track of the snow storage and fractional snow covered area during the winter and the snow melt season. GamSnow does not aspire to simulate lateral transport or distribution of snow explicitly, only a statistical representation of sub-grid snow distribution is employed. The spatial resolution (grid cell size) is therefore best selected so that net transport into or out from any grid cell is negligible. A grid size commonly used in maritime-mountainous regions is 1*1 km. In regions of dry/colder winters where snow transport may extend over long distances, the grid cell size needed for the same assumptions to hold may be several kilometres.

Simulating sub-grid snow distribution in 1*1 km grid cells is considerably more detailed than required for runoff prediction in typical hydropower catchments. It is, however, necessary in order to extract quantitative snow storage mass balance information from satellite imagery, which as is provides only snow covered area.

It is also necessary to correctly represent the surface energy fluxes in atmospheric modelling (Liston et al., 1999). Recently, remotely sensed information products on fractional snow cover have become available on a daily basis at sub-km resolution from MODIS and several other sensors.

2.1 Spatial distribution

The 2nd generation GamSnow routine is implemented within the Enki framework, and inherits from it the possible spatial distribution schemes. The typical case is a rectangular spatial grid with square cells aligned with its coordinates, but GamSnow itself does not require these restrictions. It can also be run for any list of locations; for instance subcatchments or elevation zones. GamSnow/Enki assumes all variables to be completely georeferenced, and will verify that all distributed variables share a common geodetic projection system and a common spatial geometry.

2.2 Necessary inputs

The 2nd generation GamSnow routine can be run with any time step length. It needs distributed input time series for precipitation [mm], temperature [°C] relative humidity [%], wind speed [m/s] and global radiation [W/m^2]. GamSnow does not create proxy values or otherwise respond properly to missing input values; it is assumed that such deficiencies are handled in the surrounding Enki framework. Neither does GamSnow perform any input modifications like altitude-based temperature adjustment or correction for precipitation catch deficit. The precipitation form, however, is classified as solid or liquid using a threshold temperature supplied as a calibration-enabled parameter.

A rudimentary land cover map is required as a static input, but only masked-out areas (code 0) and lakes/open water (code 1) are recognised and handled specifically in the equations. All other codes in the land cover map are simulated in the same way in both the original GamSnow and the new version presented here. Future development may extend GamSnow to taking vegetation type into account.

A map of minimum bare-ground fraction is needed, specifying for each grid cell the areal fraction that stays uncovered by snow, even at mid-winter. Usually below 0.05 except for very steep topography.

A glacier map is optional, and provides the glaciated fraction of each cell. Glaciers will only influence simulation when the snow covered fraction in a grid cell is smaller than its glacier fraction. If no map is supplied, glaciers are assumed not to exist.

In addition, 2nd generation GamSnow requires initial values for all state variables, and values for all parameters. The parameters can be chosen as either scalar values, which are available for Enki's calibration functionality, or as distributed maps in which the local values are not calibratable. Typically, the latter is chosen for parameters which can be estimated from e.g. satellite images, e.g. those in the sub-grid snow distribution.

2.3 Simulated responses

The primary response variable of the 2nd generation GamSnow routine is the simulated water outflow from the snow pack [mm]. Secondary response variables are snow covered area SCA [-] and snow albedo [-]. In addition, four effect components in the snow melt equation are exported for diagnostic monitoring; net shortwave radiation, net longwave radiation, net turbulent energy flux and energy flux from precipitation (all in [W/m^2] and positive downward).

Internally, GamSnow simulates the snow storage and its sub-grid coefficient of variation, the snow grain size, the snow surface temperature and the liquid water content of both the bulk snow pack and the topmost layer, the accumulated melt depth (since spring onset) and the magnitude of an ephemeral new-snow layer appearing on top of the distributed snow pack following spring snow events.

The Enki framework allows any exposed variable in each routine to be evaluated and used in calibration. In the current investigation, this is limited to grid cell snow covered area and catchment discharge. A range of performance criteria is available, including likelihood measures for use in estimation algorithms based on strict statistical formulation.

2.4 The melt equation

GamSnow's melt equation can best be described as an energy sum approach. In principle, it resembles a full energy balance approach, summing up the flux components net shortwave radiation, net longwave radiation, turbulent (latent and sensible) heat fluxes and precipitation heat flux (figure 1 and equation 1). Unlike a full energy balance equation however, the negative feedback mechanism represented by the snow surface temperature is not simulated. Instead, the snow surface temperature needed to estimate the upward components of longwave radiation and turbulent transfer, is simulated as a function of the wet-bulb temperature, as given by air temperature and relative humidity. This simplification avoids simulating detailed heat flux and storage within a snow pack of poorly known and highly heterogeneous depth and properties.

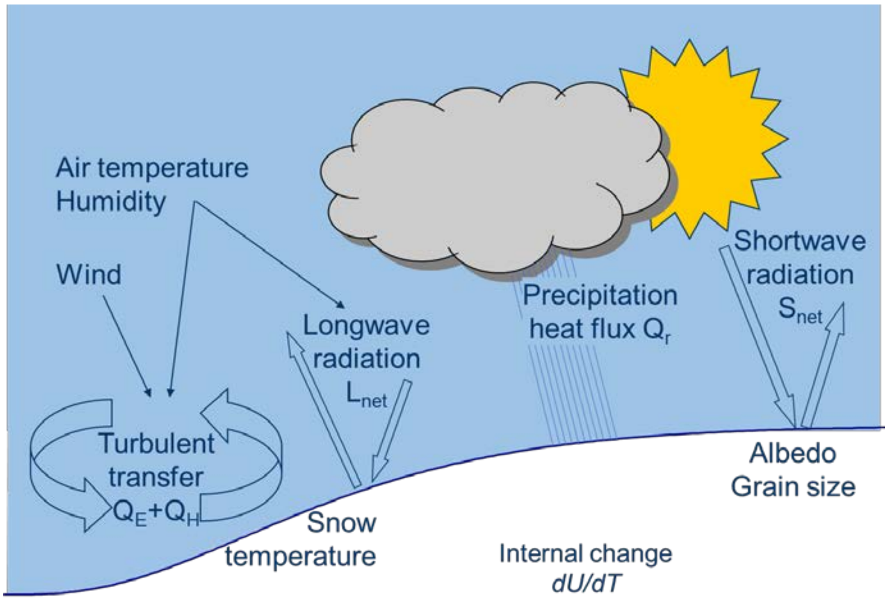

Figure 1: The forcing variables, main states, and energy terms of the snow melt equation. Ground flux and influence of clouds on short- and longwave radiation are not simulated in GamSnow.

The energy balance equation for snow melt can be formulated as (e.g. Lundquist et al., 2013):

$$Q_M = L_{net} + S_{net} + Q_E + Q_H + Q_R + Q_G - \frac{dU}{dt}$$

where Q_M is the energy flux consumed in melting snow, L_{net} and S_{net} are net longwave and shortwave radiation, respectively; Q_E and Q_H are the turbulent terms (sensible and latent heat flux), Q_R is energy flux from precipitation, Q_G is energy flux from the ground, and dU/dt is the rate of change in internal energy. All terms in [W/m^2], expressing energy flux, or rate of energy transfer per unit area.

2.4.1 Shortwave radiation

Shortwave radiation represents a large part of the energy available for snow melt; in particular in mountainous areas. Estimation of local solar radiation values is external to the second generation GamSnow as well as to the original formulation. It is usually measured as global radiation; hemisphere-integrated flux across a horizontal surface. Global radiation is a function of solar elevation, clear-sky atmospheric transmissivity, and cloud cover. The solar elevation is important, but it is known with high precision and thus not a source of uncertainty. The clear-sky transmissivity is less well known, but has a modest influence. On the other hand, the influence of clouds (fractional coverage, height and other characteristics) is both highly important and difficult to quantify using operationally available data. Improved knowledge of cloud cover properties over a region, for instance from satellite data, can therefore be of great help in creating local values for solar radiation. Shortwave radiation flux is also very dependent of the snow albedo, which represents one of the major changes in the second generation GamSnow presented here.

2.4.2 Longwave radiation

Just like shortwave radiation, longwave radiation is a net effect of incoming and outgoing components. In both versions of GamSnow, incoming longwave radiation is simulated from air temperature, with atmospheric emissivity modelled from vapor pressure. Cloud coverage is not represented. Outgoing longwave radiation is simulated as a function of snow surface temperature, assuming a snow emissivity of 1.0. The snow surface temperature driving the outgoing flux is another aspect which is changed in the new GamSnow formulation. In this case the general approach is kept, but the amount of information behind the new formulation is stronger than in the original GamSnow routine.

2.4.3 Turbulent energy flux

The turbulent energy flux consists of sensible and latent heat flux components, for which the circulation of air above the snow pack is the most important transport process. The two depend on a turbulence function, which in both versions of GamSnow is a linear transformatin of wind speed, with free parameters WindScale and WindConst. The turbulence function is multiplied with surface vs reference height gradients in temperature and vapour pressure to generate sensible and latent heat flux, respectively. It is assumed that the air immediately above the snow surface is saturated and at snow temperature. Vapour pressure is a function of temperature and relative humidity.

2.4.4 Internal energy and liquid water content

The total energy flux from the four main components is either positive or negative, and will increase or decrease the energy content of the snow surface layer. The surface layer is assumed to insulate the deeper snow pack from temperature changes, and has a thickness regulated by a free parameter. The energy content of a dry snow surface layer at 0°C is zero. Negative energy content in the surface layer means that its temperature is also negative, positive energy content that it contains liquid water. Snow surface energy content exceeding what corresponds to maximum liquid water holding capacity, is made available for snow melt in the underlying bulk snow pack. The bulk snow pack has the same maximum water holding capacity, and runoff occurs when it is exceeded. Liquid water content in the bulk snow pack can only be reduced by new snowfall, not by refreezing, since the bulk snow pack is assumed thermally insulated from the atmosphere. The bulk snowpack liquid water content therefore delays melt onset at the seasonal scale, but not at the diurnal.

2.5 Sub-grid snow distribution

The parameterisation of snow storage and spatial distribution is divided between small- and large-scale variation components, with the grid cell size separating the two. The large scale variability is maintained by each grid cell keeping track of its own mass balance, hence more or less given by the spatial variability of input forcing. The sub-grid distribution is described by a snow depletion curve (figure 2), as is used by e.g. Liston (1999) and Luce et al (1999). The SDC represents both the cumulative probability distribution of point snow storage at melt season start, and the bare-ground fraction of the grid cell as a function of accumulated melt depth throughout the spring season. A necessary condition for these to be equivalent is that snow melt intensity is spatially homogeneous within each grid cell. The only state variable active through the melt season is the accumulated melt depth (**λ**), whereas snow covered area SCA, runoff and remaining snow storage are functions of **λ**,

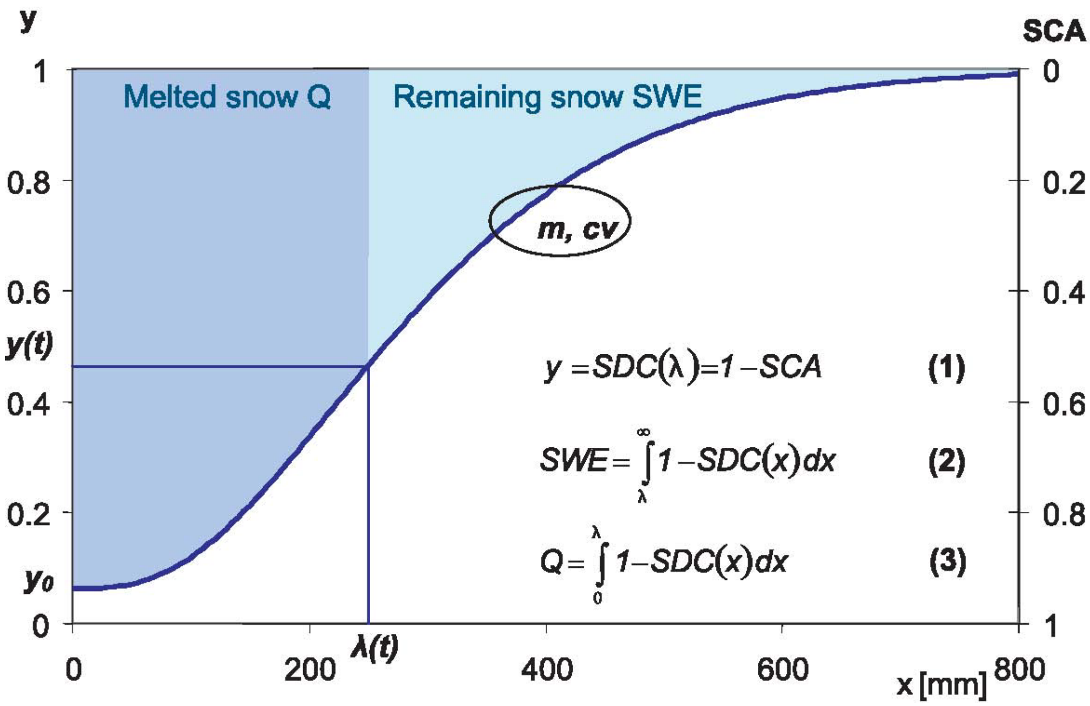

Figure 2: The snow depletion curve expressed as a cumulative probability distribution, parameterised by its mean value *m*, coefficient of variation *cv*, and the initial bare-ground fraction y_0 (from Kolberg el al., 2006). During the melt season, λ(t) is the accumulated melt depth, the functional value y(t) = 1-SCA is the fraction of bare ground, whereas the mass balance is found by integrating (1-y(x)) from 0 to λ for melted volume (dark blue); from λ to ∞ for remaining snow storage (light blue).

A parametric SDC with a limited number of parameters cannot follow all possible events. In particular when new snow falls on a partly snow covered grid cell, the new SDC will ideally have a break point at the old SCA value. This singularity cannot be represented in a 3-parameter SDC model. To avoid excessive special case handling, the SDC operates in different modes during accumulation and melt seasons, and treat each season's unusual events in a simplified manner. In winter mode, a snow melt event lowers the curve itself rather than truncating it, hence maintaining full SCA unless the storage is completely emptied. In spring mode, a snowfall event on reduced SCA generates an additional, spatially homogeneous temporary layer. All subsequent melt occurs from this temporary layer until it is emptied; only then the SCA changes back to the value it had before the melt event. These simplifications are usually active only in the edges of each season, and helps maintaining a parametrically simple SDC as a stable relation between SCA and mass balance. This in turn is a prerequisite for using satellite snow coverage data to update snow cover mas balance. It may, however, be overly crude in regions where the snow cover appears and disappears through the cold season.

In principle, any monotonous function can be used as SDC model. If the SDC is applied to a small, well-monitored catchment, it could be advantageous to increase its flexibility by adding more parameters. When applied to every grid cell in a regional model, however, the SDC should be simple and robust. This increases the probability for satellite image information to identify biases in the important mass balance state, rather than just tuning the distribution form.

Both the original and the new GamSnow use a 2-parameter Gamma distribution (hence the name), with an additional, term y_0 to account for steep ridges and slopes on which snow does not accumulate. This y_0 parameter is usually small to negligible in a pure simulation context. In updating, however, it helps avoiding drastic reduction of snow storage to comply with early-spring satellite images showing small but significant bare ground at high elevation.

Of the three SDC parameters in GamSnow, the mean value (m) is clearly season-specific. The sub-grid coefficient of variation (cv) and the all-winter bare ground fraction (y_0) are regarded as model parameters, which can be estimated as heterogeneous maps if a sufficient number of melt-season satellite images are available for a calibration period. Kolberg and Gottschalk (2010) has shown that the inter-annual stability of these parameters is high, with considerable advantages for building strong confidence. This again increases the probability that observed SCA in a real-time situation can be reliably used to update the snow storage.

2.6 Runoff from glaciers

GamSnow includes a simple mechanism for simulating glacier runoff. A glacier is represented as an infinite storage with constant spatial extent. No simulation of mass balance, varying glacier extent, or ice transport is provided. A glacier map must be supplied which for each pixel quantifies the fraction covered by glaciers. It is assumed that the seasonal snow disappears from all non-glaciated areas before the glacier ice is exposed. Hence the glaciers are only active when the SCA is lower than the glacier percentage. Melt intensity is calculated as for snow, but with a temporally constant glacier albedo value rather than the simulated snow albedo. In glaciated grid cells, remaining snow after a summer is not carried over to the next year's snow storage as in non-glaciated cells, but assumed to be lost to the glacier.

3 A new albedo formulation

In the existing GamSnow model, albedo development is simulated in dry and wet snow by using simple decay rates with two different time constants. In addition, free calibration parameters include maximum and minimum albedo as well as the amount of new snow needed to reset the albedo. Also calibrated is glacier albedo, giving six parameters in total. Even when using numerous catchments and several seasons' time series of satellite snow cover images to estimate a single parameter set, no calibration exercise has been even close to identifying clear optima for these. A strong simplification of the albedo model was thus seen as necessary to reduce the parameter equifinality and gain confidence in the optimised values (see discussions by Beven etc).

It is in the radiation terms that the main differences with respect to the original GamSnow equation is found. Incoming short wave radiation is readily available both as ground measurements and as remotely sensed values (Trigo et al, 2011); the major source of uncertainty is the albedo conceptualisation. Albedo is known to depend strongly on snow grain size (Wiscombe and Warren, 1980), the content of black carbon and other impurities, the incidence angle, and the spectral composition of the solar radiation. In particular, the reduction in albedo in ageing snow is driven primarily by the grain size growth. The dependency of incidence angle and spectral composition, however, mean that the decomposition of solar radiation into direct and diffuse components plays an important role for more than terrain correcting of incoming radiation.

3.1.1 Grain size modelling, dry snow

Flanner and Zender (2006) and Flanner et al (2007) discuss the parameterisation and development of snow grain size. Based on the concept of specific surface area (SSA or $\hat{S}$), they demonstrate that the optical properties for a collection of snow grains with different sizes and shapes can be developed theoretically for an effective grain size ratio inversely related to SSA. This is the basis for their model SNICAR; a complex, multi-layer simulator of grain size growth in dry snow. They also propose a simpler parameterisation shown to closely replicate SNICAR's results for surface grain size development, as needed in climate and snow melt models. This parameterisation appears in somewhat different transformations in various papers, the formulation used in this report coincides with the version used in Kuipers Munneke et al, 2011, and states:

$$\frac{dr}{dt} = \left(\frac{dr}{dt}\right)_0 * \left(\frac{\tau}{(r - r_0) + \tau}\right)^{1/\kappa}$$

This is a simple, 3-parameter equation for the rate of change in specific surface area. However, the three parameters are not constants, they are themselves functions of four properties of the snow cover: Temperature, temperature gradient, density and fresh snow grain size. Flanner and Zender (2006) provide these functions as lookup tables, spanning the interval -50 – 0 °C, 0 – 300 °C/m, 0 – 400 kg/m^3, and 60 – 100 m^2/kg; in 11, 31, 8, and 3 steps, respectively. The tables are available at http://snow.engin.umich.edu/snowaging/ (accessed at 2016-09-15).

The coefficients in this 4-dimensional table are tuned by minimising the sum of squared errors of the simplified equation versus the full SNICAR model over a two-week simulation period (336 hourly values). The estimation of the three parameters was done independently for each of the 8184 different combinations of the four snowpack properties (M. Flanner, personal communication 2016).

Strictly speaking, this means that the simplified SNICAR model has more than 24 000 estimated parameters. These are tuned under controlled conditions to full- SNICAR simulated values; and mostly they vary smoothly along their dimensions. In some intervals, however, the parameters as well as the resulting grain growth rate depend in a non-monotonous manner to some of its snow-property forcing, as is illustrated in figure 3. This behaviour is not realistic, and probably arises from different subsets of the 336 hourly residuals being most influential on the estimation. The assumption of unchanged forcing conditions over the 2-week period is itself unrealistic, at least for some of the value combinations.

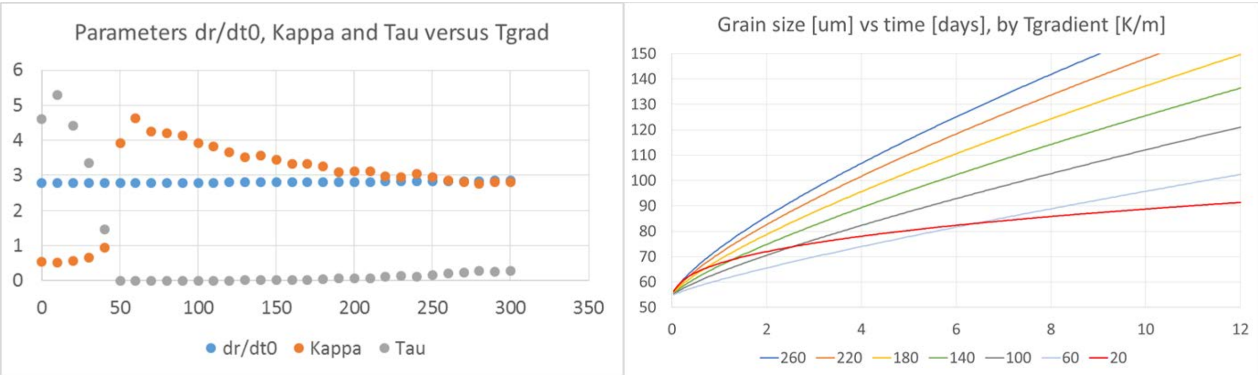

Figure 3: Non-monotony in the simplified 3-parameter SNICAR equation; parameters κ and τ versus g_T (left), and predicted grain size versus time for different g_T (right). The latter show smooth behaviour for strong gradients, but shifts abruptly as gradient decreases below 60 *K/m*.

Switching from a synthetic experiment to real-world application, the four forcing variables are in part difficult to measure and simulate. In practice they are left to simulation within the snow model which SNICAR is meant to serve; relying on all input variables used by the complete snow model. Even for a single, well-instrumented experiment plot, this is likely to induce errors well beyond those of the simplified 3-parameter equation. In particular, the uncertainty increases if the conditions include thawing and possibly refreezing of surface snow crystals.

For this reason, some effort was made to tie this formally large number of lookup-table values together in new parametric models, in which monotony could be enforced and the degrees of freedom reduced. The simplification was tuned against the simplified 3-parameter equation with lookup table values, not with respect to the full SNICAR model.

The most influential parameter is $\left(\frac{dr}{dt}\right)_0$, which dependency of snow temperature T can be expressed as 2-order polynomial

$$\left(\frac{dr}{dt}\right)_0 = AT^2 + BT + C$$

The coefficients A to C depend on the remaining snow properties g_T, S_0, and ρ; and can be modelled as:

$$A = A_0 + A_1 \cdot g_T$$

$$A_0 = 0.002835 * \ln(S_0) - 0.008411$$

$$A_1 = 3.74 \cdot 10^{-4} \cdot (0.405 - \rho) \cdot exp\left(\frac{-S_0}{28.63}\right)$$

$$B = B_0 + B_1 \cdot g_T$$

$$B_0 = 0.0051 \cdot S_0$$

$$B_1 = (0.00095\ \ln(S_0) - 0.00468) \cdot \ln(\rho) - 0.00579\ln(S_0) + 0.02842$$

$$C = C_0 + C_1 \cdot g_T$$

$$C_0 = 0.1362 \cdot S_0$$

$$C_1 = \ (0.0188 \cdot \ln(S_0) - 0.09662) \cdot ln(\rho) - 0.1109\ \ln(S_0) + 0.5706$$

where g_T is the temperature gradient, S_0 is the initial (fresh-snow) SSA, and ρ is the snow density. The modelled values for $\left(\frac{dr}{dt}\right)_0$ fit the table values to a Nash-Sutcliffe value of 0.968. It took, however, 15 parameters to reach this correspondence.

Next, we need to model the remaining parameters τ and κ in the simplified SNICAR equation. These parameters exhibit the non-monotonous dependency of snow properties, and models are therefore fitted to restricted intervals for some snow property values. The restricted snow density interval extends from 100 to 350 kg/m3, snow temperature from -30 to -5 °C, and temperature gradient from 30 to 250 °C/m. In addition, some combinations within these intervals are also removed.

The parameter τ is modelled by its natural logarithm as (Coefficients A-D are different from those above):

$$ln(\tau) = A \cdot (-T)^B \cdot \rho^2 + C \cdot g_T + D$$

where A = - 0.00001886, B = 0.756, C = 0.037, and D = -0.0193. The modelled ln(τ) values fit their tabulated counterparts to a Nash-Sutcliffe R^2 value of 0.825, for τ the R^2 value is 0.53.

The parameter κ is also modelled by its natural logarithm (again coefficients A-E are different from above):

$$ln(\tau) = A \cdot (-T)^B \cdot \rho + C \cdot g_T + D \cdot S_0 + E$$

where A = 0.000335, B = 0.734, C = - 0.00224, D = -0.00506, and E = 0.805 The modelled ln(κ) values fit their tabulated counterparts to a Nash-Sutcliffe R2 value of 0.825, for τ the R^2 value is 0.737.

The models for τ and κ has four and five parameters, respectively; one more than their number of predictor variables. They clearly do not match the performance of the 15-parameter model for $\left(\frac{dr}{dt}\right)_0$. This is reasonable given that certain aspects of the tabular values' behaviour were deliberately not included in the model, with increased residuals as an obvious result.

In total, the simplification of the simplified SNICAR model still possesses 24 free parameters. The identifiability of these is not investigated, given that the reference to which they are calibrated is itself a synthetic data set. but at least they are ensured to have monotonous influence. In a snowmelt model for temperate, seasonally snow covered regions, however, 24 free parameters is probably still an order of magnitude higher than one should expect to be identifiable within a realistic amount and diversity of calibration information. Highly uncertain and heterogeneous forcing, occasional thawing, and frequent new snow events with high small-scale variability, are all processes which may impact the development of surface reflectance more than realistic variations of snowpack density and temperature gradient.

3.1.2 Grain size modelling, wet snow

Compared to the theoretical development of a crystal growth rate model for dry snow; the models developed for simulating wet snow grain size growth has been simpler and more empirically based. “Simpler” here does not apply to the experiments, which require special techniques to keep the samples at constant wetness.

Brun (1989) conducted a laboratory experiment in which dry snow was brought to 0°C and further exposed to heat to achieve a desired liquid water content, before the sample containers were put in an insulated ice-water bath to avoid further phase change. Over the next two weeks the crystal growth rate was studied for snow samples with different liquid water content, by taking out sub-samples from the originally 7-litre samples and analysing their grain structure.

The analysis of Brun (1989) showed that the initial phase of metamorphism involved more change of crystal shape than of size; changing the specific surface area more than grain size itself, while also the snow density increased. After the initial phase, the average crystal volume increased approximately linearly with time, and with liquid water content raised to the power of 3. Beyond the maximum liquid water content of snow at approximately 9 percent by mass, percolation drained the snow and prevented further increase in both wetness and grain growth rate.

The model proposed by Brun (1989) on the basis of these investigations is then expressed in terms of grain volume as

$$v(t) = v_0 + v' \cdot t$$

$$v' = v'_0 + v'_1 \cdot L^3$$

$$v'_0 = 1.28 \cdot 10^{-8} mm^3 s^{-1}$$

$$v'_1 = 4.22 \cdot 10^{-10} mm^3 s^{-1}$$

where v_0 is the initial average grain volume in mm^3, *t* is time in seconds since this initial state, and *L* is liquid water content in percent by mass. Using the chain rule and the formula for volume of a sphere, Brun’s (1989) model can be expressed in grain radius r:

$$r(t) = r_0 + \frac{(v'_0 + v'_1 \cdot L^3)}{4\pi r^2} \cdot t$$

where v'_0 and v'_1 are as above, and *r* is in *mm*. If $v'_0/4\pi r^2$ is seen as the growth rate when L = 0 and replaced with SNICAR’s equation for dry snow, we arrive at the equation adopted by Kuipers Munneke et al. (2011), with v'_1 now named C, and L named f_{liq}.

$$\frac{dr_{e,wet}}{dt} = \frac{C f_{liq}^3}{4\pi r_e^2}$$

This approach assumes that for wet snow, the moisture-driven grain growth is added to the dry snow growth, rather than replacing it. In the 2nd generation GamSnow, C is kept as a tuneable parameter alomg with the grain size of new snow, effectively targeting the melt and accumulation season, repsctively.

The Brun (1989) model contains a strong negative feedback, in that dr/dt is proportional to r^{-2}. This means that the grain size growth quickly flattens out. Starting from a grain size of 50μm, the model reaches 378 μm (albedo=0.748) after around six days, but it takes another 25 days to reduce albedo to 0.72.

For small and intermediate grain sizes, the Brun (1989) wet growth model is highly sensitive to snow wetness, which enters the scaling raised to the power of 3. This means that for any grain size, the snow at the maximum of 10% liquid water content (lwc) grows 1000 times faster than snow with 1% lwc. For ripe snow, this high sensitivity is counterbalanced by the grain size feedback, but for fresh snow, this is a very high sensitivity to a state which difficult to simulate. Not only is production of the first melt water difficult to predict due to the uncertainty in grain size and snow pack internal energy, but the vertical distribution of this liquid water over the top snow layer interacting with radiation brings additional challenges.

Figure 4 illustrates the albedo and grain size development in Brun's (1989) model versus the exponential decay used in the original GamSnow albedo routine. We see that Brun's (1989) model rapidly reduces the albedo as the wet snow is fresh, whereas after six days it is caught up by the original formulation. The exponential model, however, quickly flattens out towards the user-set minimum albedo value, whereas Brun's model will continue (albeit very slowly) to reduce the albedo.

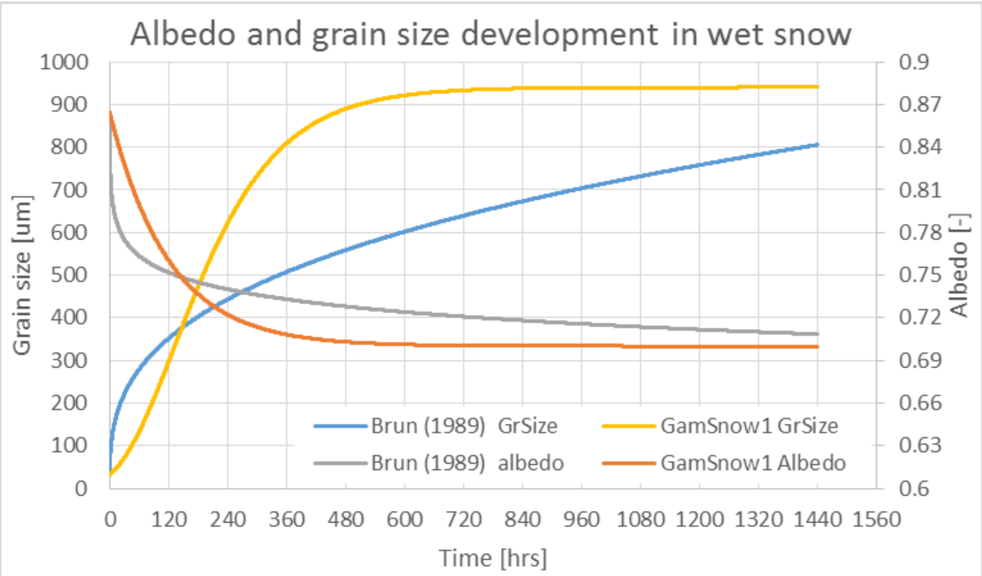

Figure 4: Grain size and albedo development over time in wet (saturated) snow in GamSnow1 and according to Brun (1989). Grain size does not appear in the original GamSnow routine, but is calculated from albedo using the inverted relation.

3.1.3 Albedo model

Based on the previously developed equations for dry and wet snow grain growth rate; Gardner and Sharp (2010) propose the following model for broad-range snow albedo:

$$\alpha = \alpha_S + d\alpha_c + d\alpha_{u'} + d\alpha_\tau$$

Here, α_S is the albedo of pure snow due to grain size only, and the additional terms describe the effect of impurities, zenith angle, and clouds, respectively. A similar model is used by Kuipers Munneke et al (2011) with some adjustments to the thinner atmosphere found in Antarctica. The four terms are modelled as:

$$\alpha_{\hat{S}} = 1.48 - \hat{S}^{0.07}$$

where $\hat{S}$ is the specific surface area;

$$d\alpha_c = max\left(0.04 - \alpha_{\hat{S}}, \frac{-c^{0.55}}{0.16 + 0.6\hat{S}^{0.5} + 1.8c^{0.6}\hat{S}^{-0.25}}\right)$$

where c is the concentration of black carbon [ppmw];

$$d\alpha_{u'} = 0.53\, \alpha_S\, (1 - \alpha_{\hat{S}})(1 - u')^{1.2}$$

where u' is an effective value for cosine of the solar zenith angle, given by:

$$u' = 0.64 \cdot x + (1 - x) \cdot u$$

where $x = min\left(1, \left(\frac{\tau}{3u}\right)^{0.5}\right)$ and u is the nominal cosine of the solar zenith angle;

$$d\alpha_\tau = \frac{0.1 \cdot \tau \cdot \alpha_c^{1.3}}{(1 + 1.5\tau)^{\alpha_{\hat{S}}}}$$

where τ is the cloud optical thickness ranging from 0 to 30, and $\alpha_c = \alpha_{\hat{S}} + d\alpha_c$. Hence, in addition to the properties of the snow surface itself (grain size and carbon concentration), this model also accounts for solar incident angle and the change in spectral composition of sunlight during cloudy conditions.

In addition to the grain size and albedo parameterisations themselves, some pragmatic choices have to be made before the model is complete: What is the SSA in fresh snow under different conditions, to what extent is grain size reset to fresh-snow value after a thin new snowfall, how does rain events or repeated freeze/thaw cycles affect the grain size, etc.

Kuipers Munneke et al (2011) set the grain size of refrozen snow to 1500 µm, admitting the arbitrariness of this choice. A special treatment for refrozen snow crystals is reasonable, since these are created and grown by freezing of water droplets, not by sublimation. In the spring snow packs of temperate regions this process is probably also ubiquitous and highly influencial, compared to the Antarctic snow pack for which the Kuipers Munneke (2011) model was developed.

However, the effect is quite dramatic, with grain size simply set to 1500 um (albedo approx.. 0.674) as soon as the snow is characterised as refrozen. In comparison, Brun's wet snow model does not reach grain size above 805 um or albedo below 0.71 even after two months with continuously saturated snow. Extreme sensitivity to thresholds is not a desirable property for a model simulating under considerable uncertainty. The most dramatic effect is not the minimum albedo, but the fact that refreezing is likely to take place during the very first night after melting has generated some liquid water available for refreezing. Effectively, this means that Brun's (1989) equation rarely comes into play when combined with the concept of refrozen grain size, since the snow usually goes more or less directly from a cold state to a refrozen state. This also means that the one free parameter in Brun's (1989) equation would be non-influential, which was confirmed during calibration attempts with this model.

This and similar assumptions add to uncertainty in parameters and forcing; and makes albedo modelling difficult, in particular when the snow melt season is also targeted.

For hydrologic model applications, it would therefore be beneficial if albedo could be measured extensively to either replace or verify the model's behaviour. Recent algorithm development based on spaceborne spectrometer information have shown good results in producing grain size estimates based on reflectivity (Painter et al., 2009).

4 Results

4.1 Experiment setup

The 2nd generation GamSnow model was evaluated against measured runoff and observed snow covered area; and compared to the original model formulation. The data set used in the comparison covers a mountainous region in western Norway, with six catchments between 11 and 110 km^2 in size. The spatial resolution was 1*1 km, temporal resolution daily, and the selected period 2009 and 2015. For precipitation and temperature, gridded values from the SeNorge data set were downloaded from the Norwegian met office and used directly. For global radiation, wind speed and relative humidity; gridded values were interpolated using Kriging.

The region is seasonally snow covered; with stable snow cover typically starting in December. Elevation ranges from 0 to 1700 m a.s.l., with tree line at approximately 1000 m a.s.l. The snow melt season usually starts in April at the low altitudes, May in the mountains. The climate is maritime, and lower-lying catchments may experience occasional runoff events during some winters.

The two models were set up in parallel within the Enki modelling platform. Apart from the two snow routines the two models were identical, using a power-law response routine based on Kirchner (2009) and no routing routine due to the relatively small catchments and daily data. The Dream algorithm (Vrugt et al, 2009) was used for estimation of posterior parameter distributions, but due to long execution times, the results did not suffice for complete distribution estimations. Instead, optimal values and the corresponding performance were noted, and plots of performance versus single-parameter values were examined visually.

The parameter set was calibrated as regional, that is, the same values were applied anywhere, meaning that the optimal parameter set is a compromise between the catchments. In addition to the discharge series, 19 images from the MODIS sensors through the 2010 melt season were used to evaluate the simulation of snow covered area. A likelihood measure was formulated and used in the Dream runs, but only traditional squared-differences based performance measures were taken out and analysed.

The two snow routine versions differed in a number of free parameters; all of which in the albedo subroutine: The original formulation included four free parameters for maximum and minimum albedo, slow and fast albedo decay rate, while the new formulation included one free parameter (wet-snow grain growth rate). Both routines had parameters for glacier albedo and new snow depth needed to reset albedo to fresh-snow value. Apart from the albedo routine, the models were identical in terms of free parameters.

4.2 Calibration results and performance statistics:

The Dream algorithm was run for around 1000 model evaluations, and seemed to have converged after approximately 500. This sample size is too small to make inference about the multivariate posterior distribution which Dream aims at. However, each parameter's approximate optimum and level of identification can be read out of the results. Overall, the new GamSnow formulation was able to reach higher performance than the traditional; evaluated by Nash-Sutcliffe R^2 for discharge Q and snow covered area *SCA*. Figure 5 shows the performance results for the two models; averaged over 6 catchments for Q, and over 19 satellite images for SCA. In addition to the better performance along both axes, the new model avoids the quite large pareto front visible for the traditional; in which there appears to be a trade-off between better discharge simulations and better SCA simulations.

However, the absolute level of the results is not highly impressive, and inspection of the six catchments from which figure 5 shows an average, indicates that there are issues with the data quality for some of the catchments.

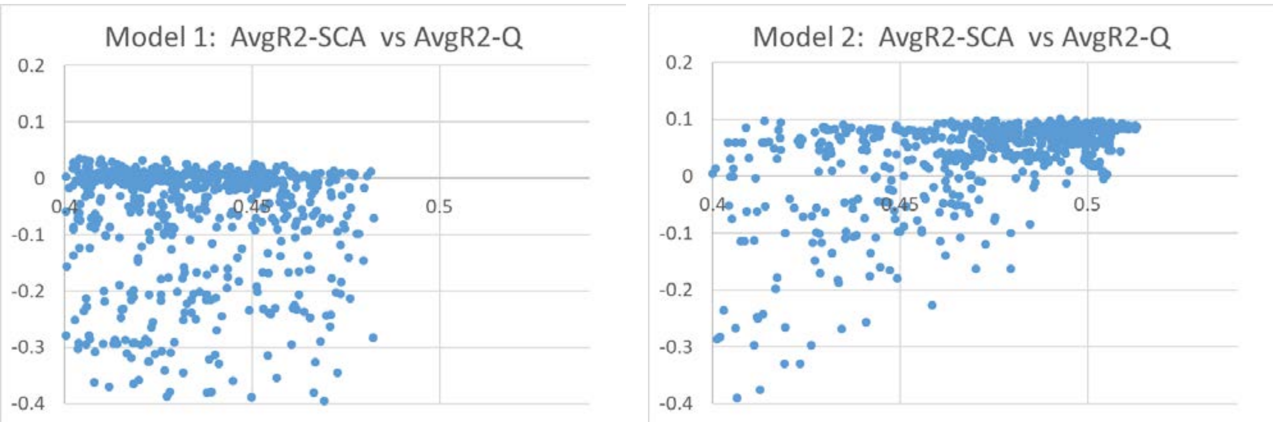

Figure 5: Pareto plots showing the combined performance for snow coverage (SCA) and discharge for the original GamSnow model (left) and the new version (right). The new model achieves higher performance for both variables. In addition, the agreement between the two criteria is better for the new model, wheras the best Q performance for the old model appear for non-optial SCA performance.

4.2.1 Identifiability of albedo-model parameters

The 2nd generation GamSnow routine has three albedo parameters, one of which unique to this routine (wet snow grain growth rate). The other two (albedo reset snowfall depth and glacier albedo) are shared by the original model. The original-model parameter most similar to the new model's wet snow grain growth rate is the fast albedo decay. Both of these regulate the metamorphosis when the snow surface is wet, hence these will be compared here.

This means that except for the response to new snowfall, the re-parameterisation of the simplified SNICAR equation replaces all calibration freedom for cold snow conditions. To some extent, this corresponds to the validation data set, which consists of spring-season SCA images and catchment runoff. Neither of these contain much information on the cold-snow behavior. Remotely sensed observations of albedo or grain size as is demonstrated using the MODSCAG algorithm (Painter et al., 2013) would improve this situation, and could possibly justify a free parameter also in the dry-snow section of GamSnow's albedo routine.

Figure 6 shows that the parameter regulating how large snowfall is required to reset the albedo to its fresh-snow value, is more or less non-influential in both models for these two evaluation criteria. Direct evaluation to albedo measurements might have shown some sensitivity, but for the two variables used in the current experiment, this parameter is redundant.

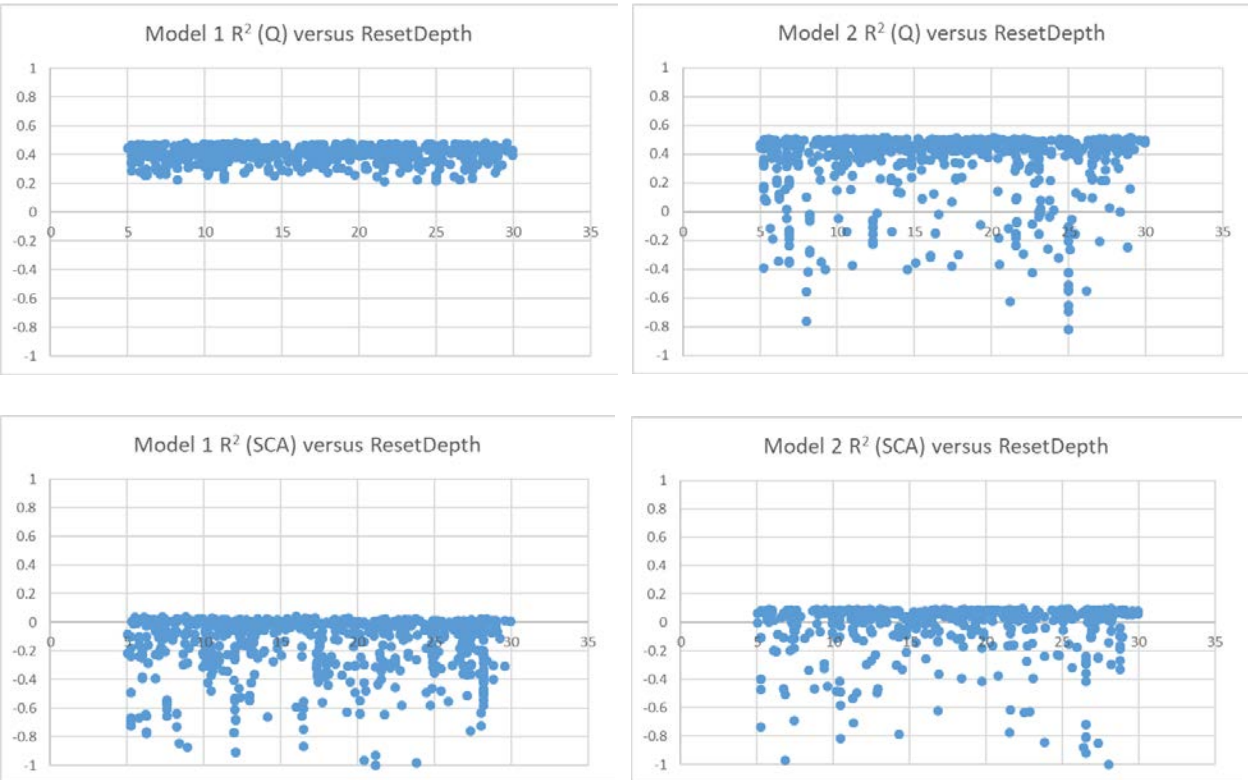

Figure 6: Model sensitivity to the albedo reset snowfall depth for old (left column) and new (right column) model; with respect to discharge (top row) and SCA (bottom row). Both models are insensitive to this parameter for both simulated variables.

Figure 7 shows how the two models respond to their respective parameters for snow metamorphosis rate during wet conditions. Note that the value in model 1 is a time scale (low values meaning rapid decay) whereas for model 2 the opposite is the case. Again, the sensitivity is low. For the new GamSnow parameterization (Model 2), a reason for insensitivity to this parameter is the grain size of 1500 μm used for refrozen snow; originally abruptly, in the current implementation asymptotically with a 1-day time scale. Since refreezing is likely to occur as soon as melt has produced some wet snow, the albedo development is very often taken over by the refreezing process, leaving the wet snow growth rate largely unused. This will be even more the case if simulation is performed for hourly time steps.

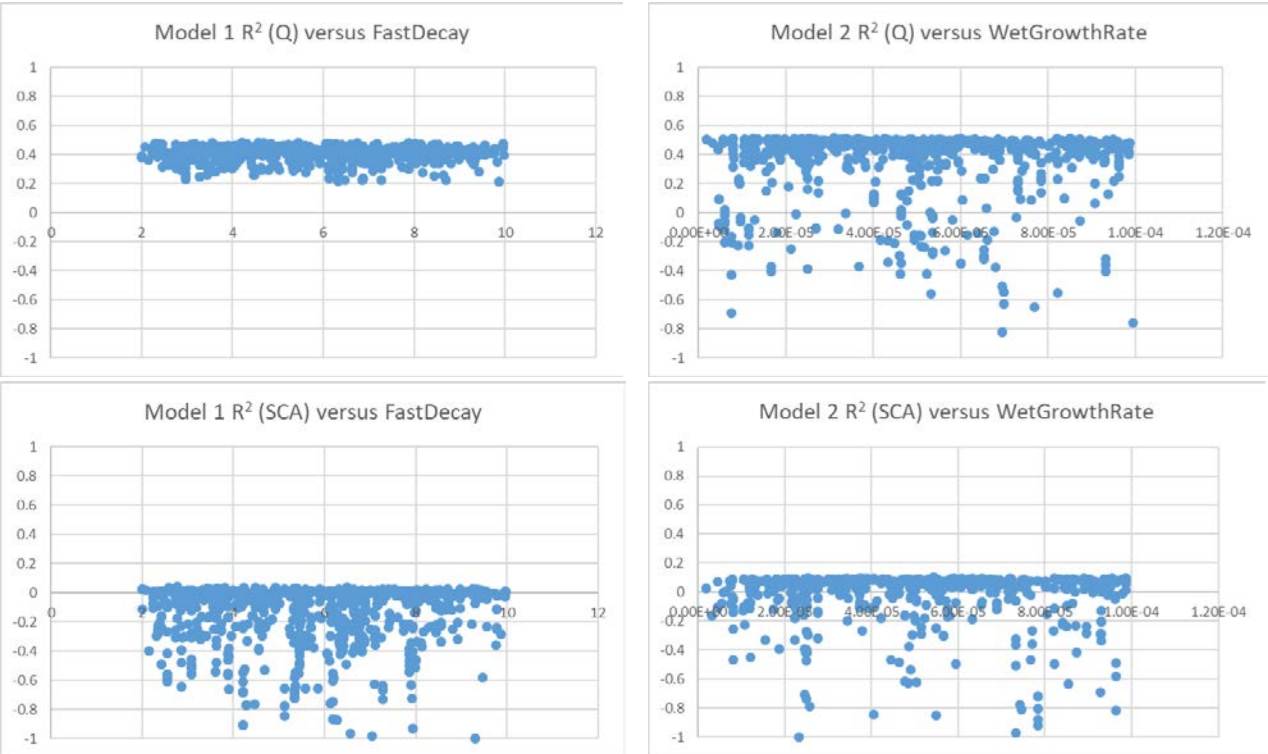

Figure 7: Model sensitivity to the wet-condition albedo decay rate for the old model (left column) and grain growth rate for the new model (right column); with respect to discharge (top row) and SCA (bottom row). Both models seem insensitive to this parameter

Figure 8 shows the original model's sensitivity to the maximum albedo value, a parameter not present in the new model. Evaluated against discharge, there is no visible sensitivity to this parameter. Evaluated against SCA, however, there is an identified optimum and a clear signal to avoid fresh-snow albedo values above 0.9. The optimum is not very strong, the y axis has been stretched to highlight the variation.

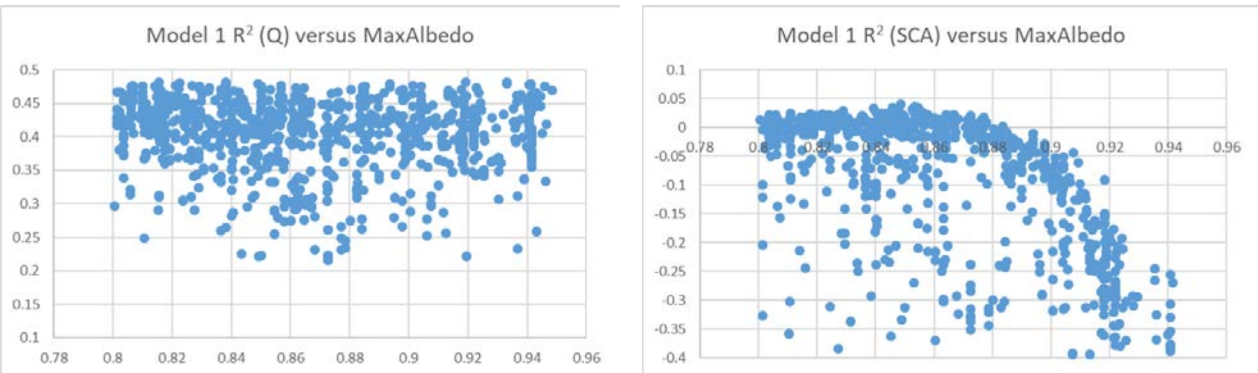

Figure 8: Model 1 sensitivity to maximum albedo value; with respect to discharge (left) and SCA (right). Model 2 has no such parameter similar. Note that the y scales are stretched to emphasise the differences. This parameter is redundant with respect to Q, but SCA evaluations show a preference for values around 0.85, most notable towards the higher end.

Not shown, and not represented in model 2 are the minimum albedo value, which shows a barely visible preference for low values, and the slow albedo decay rate, which appear redundant for both criteria.

The last albedo parameter is the glacier albedo. Three of the catchments have substantial glaciated area percentages (30% - 45%), which produce melt water at a higher rate than snow during the entire summer. However, the identifiability of the glacier albedo parameter is not very strong (figure 9), even when shown only for the catchment Lunde, which has the highest glacier coverage (45%). For SCA, the parameter is redundant in both models. A possible reason for limited sensitivity is that the glaciers are located at high elevation, where snow may persist through most of the summer. A reason for the difference between the models is that Model 1 albedo very quickly levels out at its minimum value, whereas the new model's albedo stays well above the glacier albedo during most of the summer, and hence is more influenced by the markedly lower glacier albedo. The redundancy with respect to SCA is obvious, since neither model's SCA predictions are influenced by the glacier albedo in any way.

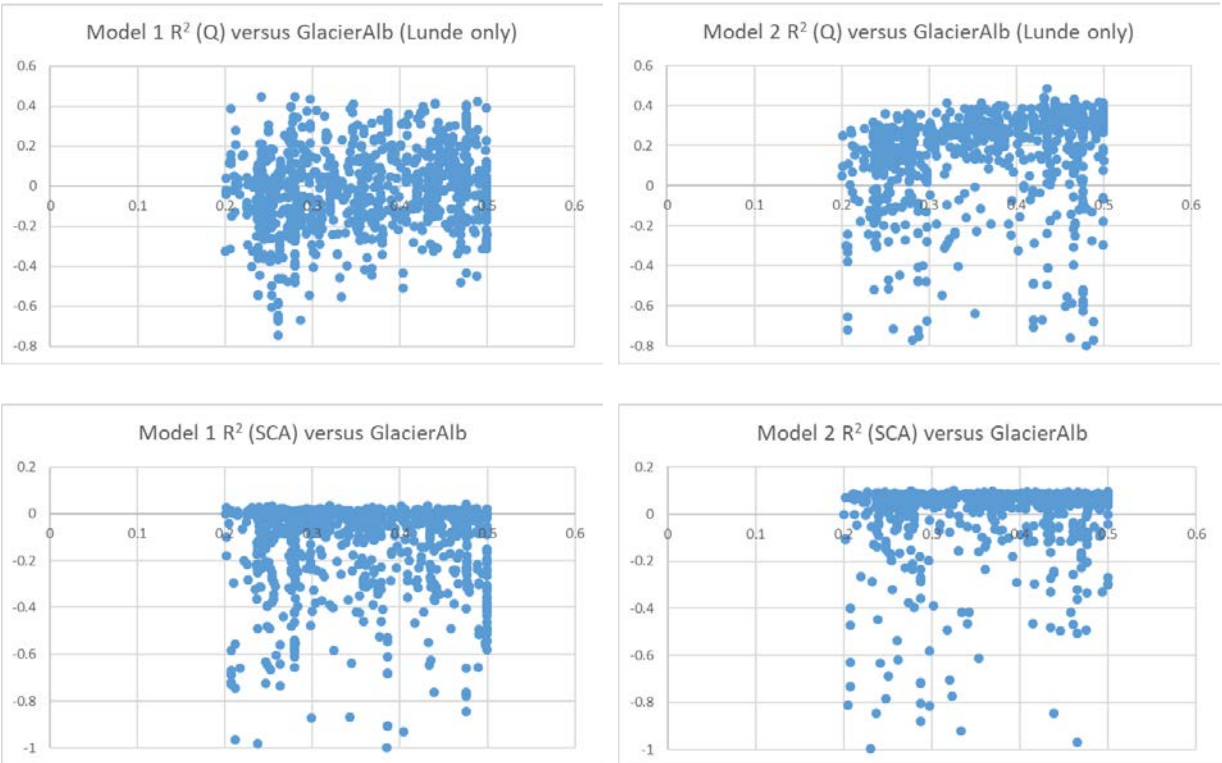

Figure 9: Model sensitivity to the glacier albedo parameter for the old (left column) and the new (right column) model; with respect to discharge (top row) and SCA (bottom row). The old model seems insensitive to this parameter, the new show a slight preference for high values in discharge simulation, no preference for SCA simulation.

4.2.2 Identifiability of other snow model parameters

Just as the albedo reset snowfall depth, the thickness of the thermodynamically active surface snow layer appears to be redundant for simulating both of the evaluated variables (not shown). This could possibly have been different if this energy content regulated the snow surface temperature (SST) as it does in reality, but in both versions of GamSnow, SST is simulated independently of snowpack state. The only effect of this variable is on the liquid water content which regulates the grain size ageing in Model 2, and on each day's time from melt onset to runoff start, which is not well represented under daily time steps.

The last snow parameter, apparent in both models, is the wind speed sensitivity in the turbulence function governing both sensitive and latent heat flux. Figure 10 shows that this sensitivity is very high for the new model, with respect to both evaluated variables. The dramatic difference between the models arises because in the new model, this is the only parameter effectively regulating the overall melt intensity, whereas the old GamSnow formulation has several parameters available with the same potential. When viewed by their marginal distribution as here, the inter-parameter dependency and possible conditional identifiability is hidden behind the apparent redundancy.

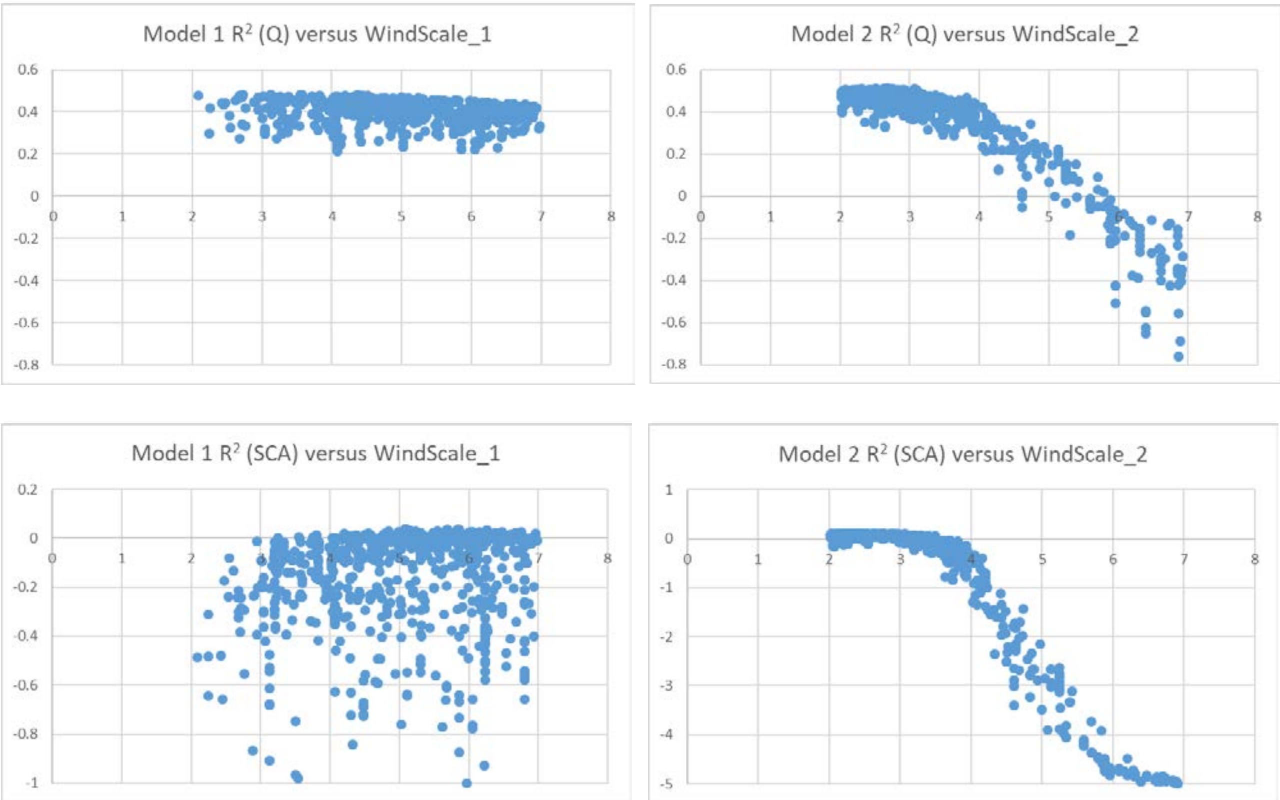

Figure 10: Model sensitivity to the wind speed scaling in the turbulent flux terms, for the old (left column) and the new (right column) model; with respect to discharge (top row) and SCA (bottom row). The old model shows a weak sensitivity to this parameter, whereas the new model is dramatically sensitive regarding both Q and SCA. Note the different axis scales.

4.3 Differences in albedo model behaviour

The largest change between the two GamSnow model versions is the albedo model, which in the new formulation has a stronger physical basis. In particular this means that the link between albedo and snow grain size is explicitly simulated, but also that the model now represents the effects of solar elevation on radiation penetration, and cloud cover on the spectral composition. Figure 11 illustrates how the two models differ, displaying catchment-average albedo for one of the basins in the investigation (the other catchments exhibit similar behavior).

The first feature to note is the considerably higher summer albedo values in the new model. This is partly because the old model's minimum albedo in this case is set to its lowest recommended value of 0.6, but also because the new model takes the solar elevation and cloud cover into account. The region is located around 62°N, and the solar elevation is far from zenith, in particular when averaged over the daily time step. The small-scale variability during the summers arises from varying cloud cover, and would be considerably larger for hourly data when also solar elevation variability contribute.

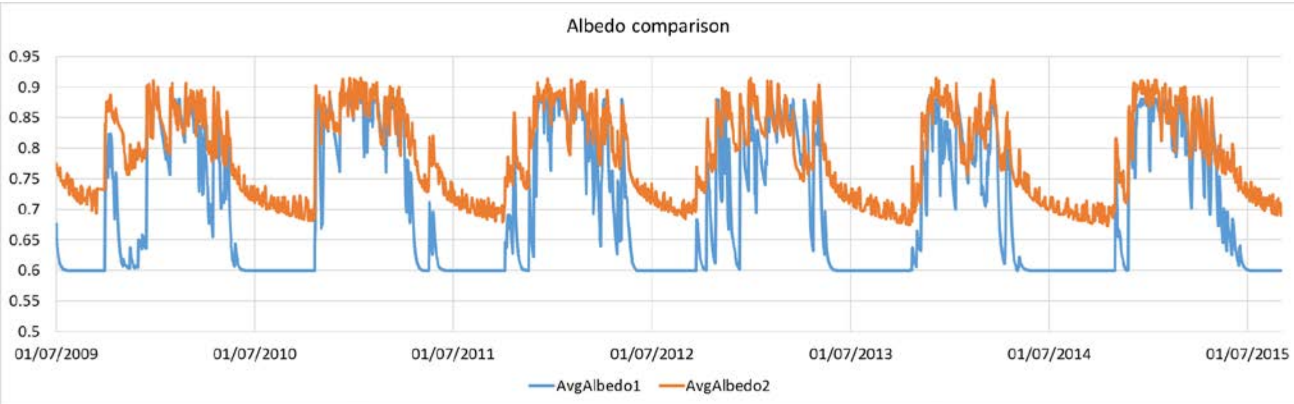

Figure 11: Albedo simulated by the original and the new GamSnow model

In the current implementation, the model does not limit the grain size to the 1500 µm set for refrozen snow, but continues to grow the crystals during the summer. This may be disputable, but without it, the continued albedo decay after July 1 would probably not occur, and the difference between the models would be even larger.

During the winter, the difference between the models are smaller. The new model shows lower small-scale variability than the older, and in particular it shows less probability of low albedo values during the winter.

4.4 Differences in longwave parameterization

In a full energy balance model, the snow surface temperature needed to calculate the longwave radiation and turbulent flux terms is simulated from the snow cover energy content. This requires a good representation of the thermal conductivity and the temperature depth profile of the snow cover, as well as high-quality forcing data. For a grid cell typically located many km away from the nearest weather station, these are unrealistic requirements. It is also doubtful that the involved processes would be meaningfully represented for daily simulation, with temporal disaggregation and sub-stepping as a necessary remedy. Instead, the original GamSnow model simulated the snow surface temperature *SST* from air temperature using a simple regression model:

$$SST_{old} = min(0.0\,, 1.16 * T_A - 2.09)$$

with T_A being *2m* air temperature in *°C*. This is a robust approach, avoiding some of the difficulties of process-based simulation of the snow cover energy dynamics. A similar approach is evaluated by Raleigh et al., (2013) who compare air temperature, wet-bulb temperature and dew point as direct predictors for snow surface temperature (with no regression model or bias correction). They analyse data from 7 weather stations in different climatic regions, which is a vastly better information basis than the single-site, single-season data set behind the model applied in the original GamSnow. Their conclusion is that wet-bulb temperature provides the best correlation to measured snow surface temperature, but that dew point produces the smallest RMS errors due to lower bias. In addition, the wet-bulb temperature bias shows smaller variability among the sites than the dew point bias, although the latter is centered around zero.

In the new GamSnow formulation, an expected bias of 4°C as extracted from Raleigh et al. (2013) is compensated for, and the wet-bulb temperature is selected as basis for snow surface temperature estimation:

$$SST_{new} = min(0.0\,, T_W - 4.0)$$

This SST model will yield lower values than the old T_A-based regression equation as long as the air temperature is above approx. -12°C for moisture-saturated air. Dryer air lowers this threshold. For the climate of this region, this model change will increase the outgoing (and thus also the net) longwave flux under most conditions. When the snow pack is at 0°C, however, the two models are equivalent.

Figure 12 shows catchment-average simulated values for net longwave radiation, for the old and the new parameterization. The incoming longwave radiation is identical in the two models, as is the outgoing radiation when the snow temperature is at its 0°C border. Hence, from the time in spring when the entire catchment is melting, the two models produce the same. As expected, the new SST model lead to less negative net longwave flux during the entire winter, compared to what the old SST model predicted.

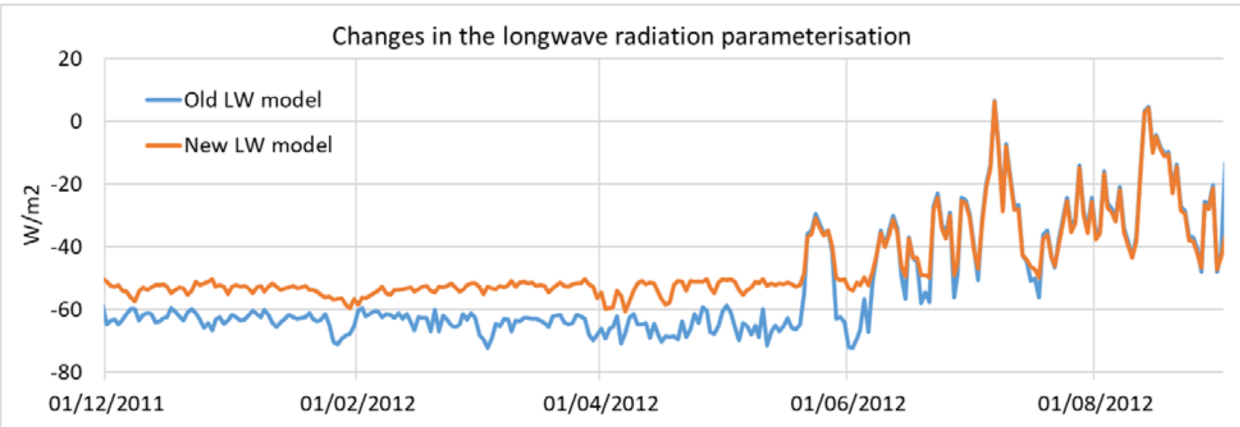

Figure 12: Catchment average net longwave flux using the old (blue) and new (orange) mechanism for estimating snow surface temperature. The new version's net radiation is generally larger or equal to that of the old model.

4.5 Hydrological simulations

Figures 13 and 14 show simulated states and responses during 01.09.2009 to 01.09.2012 for the old GamSnow (Model 1) and the new version (Model 2). The old model is a bit more likely to produce runoff events during the cold season, losing a bit more snow. Overall, however, the two models make quite similar predictions, the difference is not larger than parameter variability within the equifinality of each model could produce.

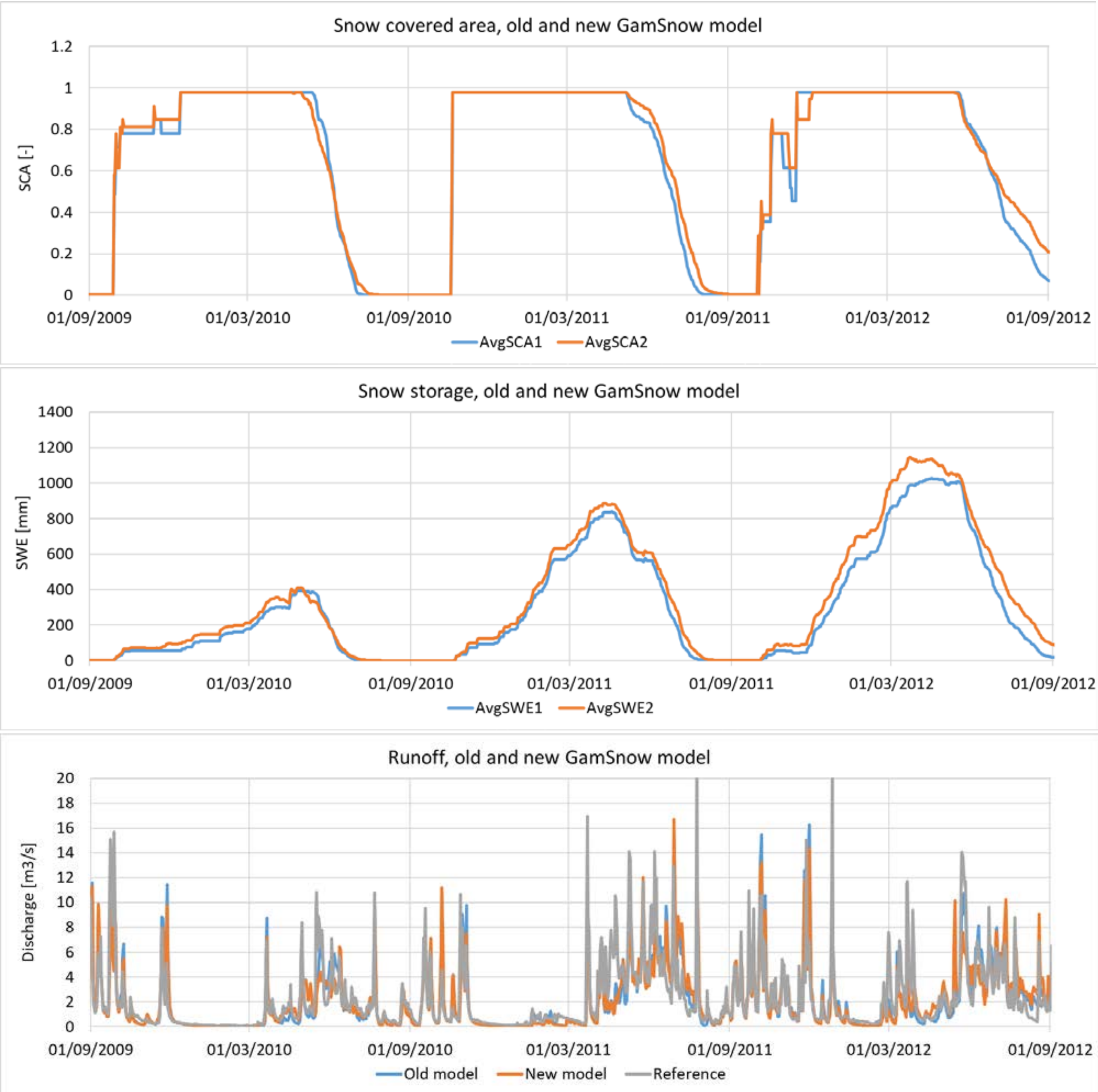

Figure 13: Water balance components for catchment Nessedalselv during 01.09.2009-01.09.2012.

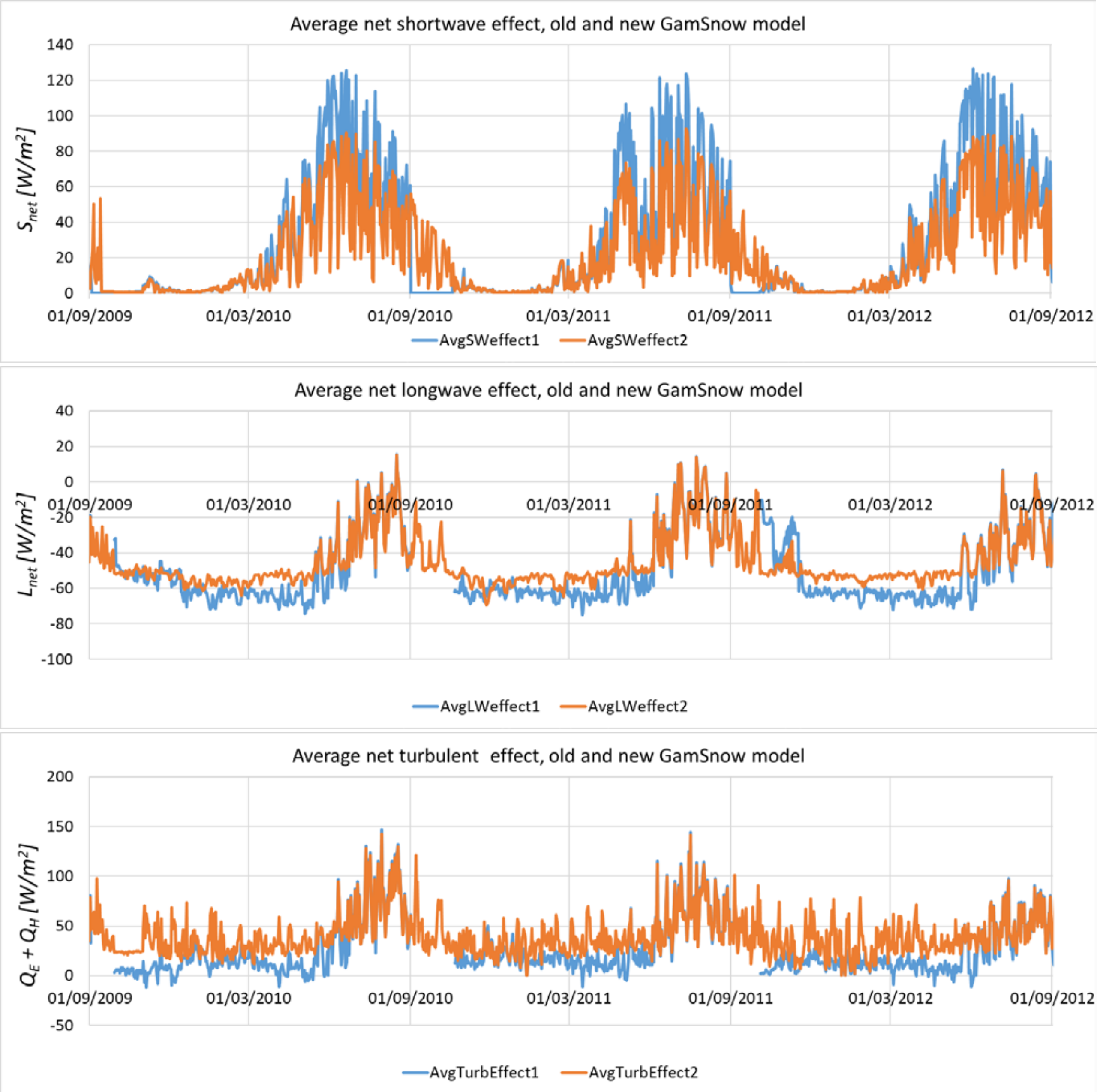

Figure 14: The major energy terms for the same period and catchment as in figure 13. We see that the shortwave fluxes are higher in the old model (1) than in the new (2), and that the opposite is the case for longwave and turbulent fluxes in the cold seasons. Note that GamSnow1 does not calculate these averages in the period from snowpack reset at September 1 until the new snow season starts.

It is worth noticing that shortwave radiation has its highest values concentrated earlier in the season than the temperature-driven energy components. This is a typical feature of maritime climates where the highest average temperatures usually occur in July and August; 1-2 months after solar radiation maximum.

5 Conclusions

The changes to the GamSnow routine, motivated by increased physical coherence and less dependency on calibration, have provided better fit to measurements than the traditional formulation. The improvement is not dramatic, and must be seen in the context of rather mediocre absolute values. Still they encourage a broader set of experiments and further improvement of input and validation data to increase the confidence. Satellite-based estimates of both short- and longwave incoming radiation may be one source of improved data; remotely sensed snow surface temperature and grain size another. These are all available data sets, most of which in operational state.

More important than the performance increase is the fact that these improvements are produced by a considerably lower number of free parameters; the flexibility being replaced by better physical knowledge. This indicates that physically based modelling can avoid the tendency of being overly sensitive to poorly known quantities, and justify its use both in operational water management and in climate studies where stationarity is questionable.

A side effect of fewer parameters is that the ones remaining tend to be better identified. In this investigation, this is clearly the case for the wind sensitivity in the turbulence function which govern sensible and latent heat flux calculation. Given that no attempt is made to modify the wind data according to exposure or sheltering characteristics, there is no reason to expect this parameter to be stationary in space.

Another positive tendency in the results is that the pareto front created by the performance in terms of discharge and snow coverage has been markedly reduced in the new model compared to the original. This means that different validation data agree on which parameters are optimal, which in turn gives confidence in the model structure. It also suggests that the model is likely to profit from updating; a feature not always present in heavily calibrated models. This, however, has not been tested in the current investigation.

Acknowledgements

The current research and the SnowHow project has been financed by the Norwegian Research Council, KLIMAFORSK programme, under the contract no. 244153,and by the Norwegian hydropower companies E-CO, Hydro, Trønderenergi, and GLB.

Table of coefficients for the SNICAR model have been provided by Mark Flanner, along with personal help.
MODIS data have been provided by NASA EOSDIS, downloaded from worldview.earthdata.nasa.gov.
SeNorge gridded precipitation and temperature time series are provided from met.no.
Radiation, wind, and relative humidity data have been provided by LMT at NIBIO.
Discharge data have been provided by NVE.

References:

Bergström, S. and A. Forsman (1973): Development of a conceptual deterministic rainfall-runoff model. Nordic Hydrol. 4, 147–170.

Beven, K. J. (2006): A manifesto for the equifinality thesis. Journal of Hydrology 320, p. 18–36

Brun, E. (1989), Investigation on wet-snow metamorphism in respect of liquid-water content, Ann. Glaciol., 13, 22–26.

Durand, M., N. P. Molotch, and S. A. Margulis (2008), Merging complementary remote sensing datasets in the context of snow water equivalent reconstruction, Remote Sensing Environ., 112(3), 1212–1225.

Flanner, M. G., and C. S. Zender (2006): Linking snowpack microphysics and albedo evolution, J. Geophys. Res., 111, D12208, doi:10.1029/2005JD006834.

Flanner, M. G., C. S. Zender, J. T. Randerson, and P. J. Rasch (2007): Present-day climate forcing and response from black carbon in snow. J. Geophys. Res., 112, D11202, doi:10.1029/2006JD008003.

Gardner, A. S., and M. J. Sharp (2010): A review of snow and ice albedo and the development of a new physically based broadband albedo parameterization. J. Geophys. Res., 115, F01009, doi:10.1029/2009JF001444.

Kirchner, J. W. (2009), Catchments as simple dynamical systems: Catchment characterization, rainfall -runoff modeling, and doing hydrology back-ward, Water Resour. Res., 45, W02429, doi:10.1029/2008WR006912.

Kolberg, S. A., H. Rue, and L. Gottschalk (2006): A Bayesian spatial assimilation scheme for snow coverage observations in a gridded snow model. Hydrol. Earth Syst. Sci., 10(3), 369–381.

Kolberg, S and L. Gottschalk, 2010: Interannual stability of grid cell snow depletion curves as estimated from MODIS images. Water Resources Research vol. 46, doi: 10.1029/2008WR007617.

Kuipers Munneke, P., M. R. van den Broeke, J. T. M. Lenaerts, M. G. Flanner, A. S. Gardner, and W. J. van de Berg (2011): A new albedo parameterization for use in climate models over the Antarctic ice sheet, J. Geophys. Res., 116, D05114, doi:10.1029/2010JD015113.

Liston, G.E. (1999): Interrelationships among Snow Distribution, Snowmelt, and Snow Cover Depletion: Implications for Atmospheric, Hydrologic, and Ecologic modelling. Journal of Applied Meteorology, vol. 38, s. 1474-1487.

Liston G. E, R. A. Pielke Sr, E. M. Greene (1999): Improving first order snow-related defciencies in a regional climate model. J Geophys Res 104(D16): p. 19559 - 19567

Luce, C.H., D. G. Tarboton and K. R. Cooley (1999): Sub-grid parameterization of snow distribution for anenergy and mass balance snow cover model. Hydrological Processes 13, s. 1921-1933.

Lundquist, J. D., S. E. Dickerson-Lange, J. A. Lutz and N. C. Cristea (2013): Lower forest density enhances snow retention in regions with warmer winters: A global framework developed from plot-scal observations and modellig. Water Resources Research vol. 49, p. 6356-6370, doi: 10.1002/wrcr.20504.

Painter, T. H., K. Rittger, C. McKenzie, P. Slaughter, R.E. Davis and J. Dozier (2009): Retrieval of subpixel snow covered area, grain size and albedo from MODIS. Remote Sensing of Environment 113, p. 868-879.

Raleigh, M. S., C. C. Landry, M. Hayashi, W. L. Quinton, and J. D. Lundquist (2013): Approximating snow surface temperature from standard temperature and humidity data: New possibilities for snow model and remote sensing evaluation, Water Resour. Res., 49, doi:10.1002/2013WR013958.

Trigo, I. F., C. C. DaCamara, P. Viterbo, J.-L. Roujean, F. Olesen, C. Barroso, F. Camacho-de Coca, D. Carrer, S. C. Freitas, J. García-Haro, B. Geiger, F. Gellens-Meulenberghs, N. Ghilain, J. Meliá, L. Pessanha, N. Siljamo, and A. Arboleda (2011): The Satellite Application Facility on Land Surface Analysis. Int. J. Remote Sens., 32, 2725-2744, doi: 10.1080/01431161003743199

Vrugt, J., CJF ter Braak, CGH Diks, B. Robinson, J. Hyman, D. Higdon (2009): Accelerating Markov Chain Monte Carlo Simulation by Differential Evolution with Self-Adaptive Randomized Subspace Sampling. International Journal of Nonlinear Sciences and Numerical Simulation, Volume 10, Number 3, March 2009, pages 271-288.

Wiscombe, W. J., and S. G. Warren (1980), A model for the spectral albedo of snow. I: Pure snow, J. Atmos. Sci., 37, 2712–2733.

Technology for a better society

www.sintef.no